Pergamon

Tetrahedron Vol. 51, No. 32, pp. 8853-8862, 1995
Elsevier Science Ltd
Printed in Great Britain
0040-4020/95 $9.50+0.00

0040-4020(95)00487-4

On the Equilibrium between Hetareno-annulated 1,2-Dithiines and 12-Membered Cyclic Bis(butadiendiyl) Disulfides. NMR and Molecular Modelling Studies ☆

Werner Schroth [a]*, Dieter Ströhl [a], Iris Thondorf [b], Wolfgang Brandt [b], Michael Felicetti [a], Thomas Gelbrich [c]

a) Institut für Organische Chemie der Martin-Luther-Universität Halle-Wittenberg, Postfach, D-06099 Halle (Saale)
b) Fachbereich Biochemie/Biotechnologie der Martin-Luther-Universität Halle-Wittenberg, Postfach, D-06099 Halle (Saale)
c) Institut für Anorganische Chemie der Universität Leipzig, Linnéstraße 3, D-04103 Leipzig

Abstract: The oxidation of the „leuco“ indigo precursors **1** affords, depending on the nature of the annulated heterocycle, 1,2-dithiines **2** or 12-membered cyclic bis-disulfides („dimers“) **3**, respectively. An equilibrium can exist between **2** and **3** in solution which has been investigated by means of NMR and molecular modelling studies in one instance (X = O). **3** has been characterized by X-ray analysis. In the case of X = S however, only the „monomeric“ 1,2-dithiine of type **2** exists in solution.

INTRODUCTION

Thioxoindigo compounds **A**, X = NH, NCH_3, O, S, increasingly attract attention with regard to structure-colour relationships. However, all attempts to synthesize **A** have hitherto failed and raised doubts as to the ability of such compounds to exist.[1] Recently, the structure of a dithioxoindigo like system has been investigated by Gompper et al. by X-ray analysis.[2]

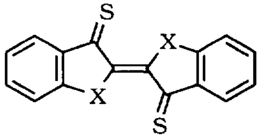

A

In our recent work[1] the oxidation of the "leuco" precursors **1** gave no **A**, X = S, O, but other products depending upon the nature of the heteroatom X. Thus, for X = S the (benzo[b]thieno)-anellated 1,2-dithiine **2a**, a valence isomer of (Z)-**A**, X = S, was the sole product.[1,3] By contrast, the corresponding oxygen analogue did not yield **2b** but the 12-membered cyclic bis(butadiendiyl) disulfide **3b** (in the solid state)[1a] whose structure has now been proved by X-ray crystallography. The latter compound formally represents a dimer of **2b**. Both these results, the formation of **2a** and **3b** are in accord with the well known preference for enthiol structures over thioxo units, here additionally favoured by the aromaticity of the heterocyclic rings.

1-3	X
a	S
b	O

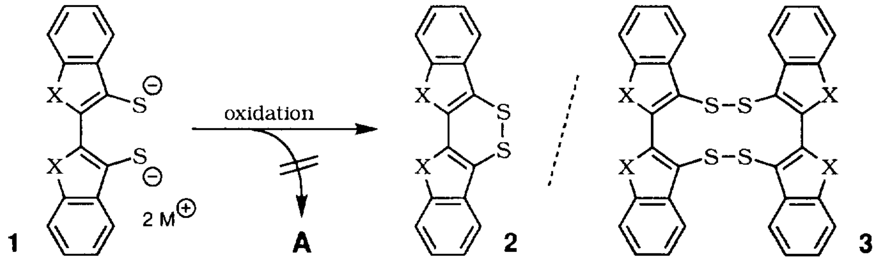

Analogously, the oxidation of 2,2'-bi(3-mercapto-1-methylindol) (**1**, X = N-Me),[1a] of 3,3'-bi(2-mercapto-1-methylindol),[1b] and of 3,3'-bi(4,5-dimethyl-2-mercaptothiophen)[1b] produced the corresponding 12-membered cyclic bis(butadiendiyl) disulfides. These unusual findings prompted us to undertake more detailed studies of **2a** and **3b** by various NMR methods and molecular modelling techniques.

RESULTS AND DISCUSSION

The X-ray analysis of **3b** reveals an unit cell with two sorts of slightly different symmetry independent molecules which each exists in an enantiomeric form. As illustrated by Figure 1[4-6] the 2,2'-bi(benzo[b]furan) units are twisted and have a sandwich-like arrangement with a distance to each other of about 4 Å. A comparison with „molecular pincers“[7] or „molecular clips“[8] is suggested. The plains of the benzo[b]furan-2-yl parts are twisted by other around 24° to each other. The disulfide bridges are centers of helical chirality[9] whilst the bihetaryl units have axial chirality due to the hindered rotation around the central C1-C9 bond. This combination of two chirality centers is comparable with that described for 4,5;6,7-dibenzo-1,2-dithia-cyclooctadiene[10] and for the 3*H*,7*H*-naphtho[1,8-*de*]-1,2-dithiepine.[11]

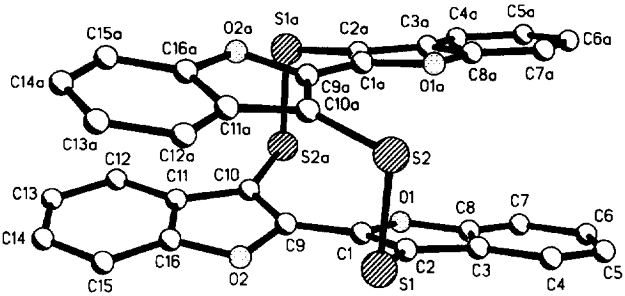

Figure 1. X-ray crystal structure[5] of bis{2,2'-bi(benzo[b]furan)-3,3'-diyl} bis(disulfide) (**3b**).

Selected data – *bond lengths:* S1-S2 = 2.066 Å, S1-C2 = 1.740 Å; *bond angles:* C2-S1-S2 = 100.6°, C1-C2-S1 = 127.6°, C3-C2-S1 = 126.5°, C1-C2-C3 = 105.9°; *torsion angles:* C1-C2-S1-S2 = -94.1°, C2-S1-S2-C10a = 74.9°, S1-S2-C10a-C9a = -91.9°, S2-C10a-C9a-C1a = -0.3°, C10a-C9a-C1a-C2a = 156.1°.

On the other hand the ^{1}H and ^{13}C NMR spectra of **3b** at ambient temperature show two sets of signals of different intensities which seems to be inconsistent with the homogeneous structure in the solid state. Moreover, with increasing temperature a significant reversible change in the signal ratios without any line broadening or coalescence, respectively, was observed. An equilibrium between two or more conformers should not be responsible for that in view of the 12-membered ring. In contrast, the ^{1}H and ^{13}C NMR spectra of **2a** consist of a single set of signals which are unaltered at higher temperature.

The ^{1}H and ^{13}C NMR data of the compounds **2a** and **3b** obtained at room temperature are depicted in the Tables 1 and 2. Due to the high symmetry four aromatic proton signals showing an ABCD splitting pattern as well as eight carbon signals are observed for both compounds. In the ^{1}H NMR spectrum of **3b** two sets of signals are present in a ratio of 65:35. For simplicity, we have labeled the two species responsible for the two sets of signals „**MA**“ (the major species) and „**MI**“ (the minor one).

The assignment of signals was carried out in the following way: First of all, the proton and carbon signals of **3b** were inspected with respect to the signal intensities and classified as belonging to either **MA** and **MI**. Then, the carbon signals were assigned for both compounds by the attached proton test (APT) and incremental calculations.[12,13] From this assignment the chemical shifts of the protons were derived by C,H COSY experiments which are also in agreement with the H,H COSY spectra. The C,H COSY spectrum of compound **3b** is shown in Figure 2.

Table 1. Chemical shifts of the protons and carbon atoms and coupling constants[a)] of the room temperature ^1H and ^{13}C NMR spectra[b,c)] of compound **3b**. The numbering of the atoms follows the scheme:

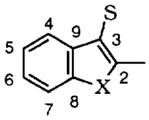

Species **MA**				Species **MI**			
^1H NMR	$^3J_{H,H}$	^{13}C NMR		^1H NMR	$^3J_{H,H}$	^{13}C NMR	
7.89 (H4)	$^3J_{4,5} = 7.5$	148.8 (C2)	115.6 (C3)	7.74 (H4)	$^3J_{4,5} = 7.7$	145.6 (C2)	109.7 (C3)
7.58 (H5)	$^3J_{5,6} = 7.3$	120.2 (C4)	125.0 (C5)	7.52 (H5)	$^3J_{5,6} = 7.3$	120.9 (C4)	125.3 (C5)
7.28 (H6)	$^3J_{6,7} = 8.2$	128.3 (C6)	111.2 (C7)	7.60 (H6)	$^3J_{6,7} = 8.1$	127.6 (C6)	112.7 (C7)
6.74 (H7)		154.1 (C8)	128.6 (C9)	7.91 (H7)		155.1 (C8)	125.2 (C9)

a) $^4J_{H,H}$ and $^5J_{H,H}$ couplings could not be observed due to line broadening
b) all chemical shifts in ppm and coupling constants in Hz

Table 2. Chemical shifts of the protons and carbon atoms and coupling constants of the room temperature ^1H and ^{13}C NMR spectra [a,b)] of compound **2a**.

^1H NMR	$J_{H,H}$		^{13}C NMR	
7.79 (H4)	$^3J_{4,5} = 8.1$	$^3J_{5,6} = 7.1$	134.0 (C2)	120.8 (C3)
7.45 (H5)	$^3J_{6,7} = 8.1$		123.4 (C4)	125.4 (C5)
7.38 (H6)	$^4J_{4,6} = -1.4$	$^4J_{5,7} = -1.1$	125.8 (C6)	122.7 (C7)
6.74 (H7)	$^5J_{4,7} = 0.7$		138.5 (C8)	136.9 (C9)

a) all chemical shifts in ppm and coupling constants in Hz
b) for the designation of the atoms see scheme in Table 1

Interestingly, besides different *intensities* of the proton signals there are also distinct *chemical shift differences* between the two species **MA** and **MI**. For instance, the H7 proton of **MA** is shifted to high field by 1.17 ppm compared with the H7 proton of **MI** whereas the H6 proton of **MI** is shifted merely 0.32 ppm to high field in comparison with the H6 of **MI**. From a consideration of the the structure of **3b** obtained by force field calculations (see Figure 3) it can be concluded that the H7 and H6 protons are shielded by the electronic ring current of the neighbouring benzene ring. The distance between the H7 proton and the centroid of the benzene ring in the force field optimized conformer is 3.15 Å. The substitution of this value (R) in equation (1)[14]

$$\Delta\delta = -\frac{\mu_0}{4\pi}\frac{e^2r^2}{2m_eR^3} \tag{1}$$

(where e is the elementary charge, r the ring radius, m_e the electron mass) allows the estimation of the chemical shifts caused by ring current thus leading to a value of 0.89 ppm for the shielding. For H6 a distance of 4.03 Å corresponding to a shielding of 0.42 ppm was obtained. The good agreement of the calculated shieldings with the chemical shift differences for H7 and H6 led us to the conclusion that these protons cannot be significantly influenced by ring current in the species **MI**.

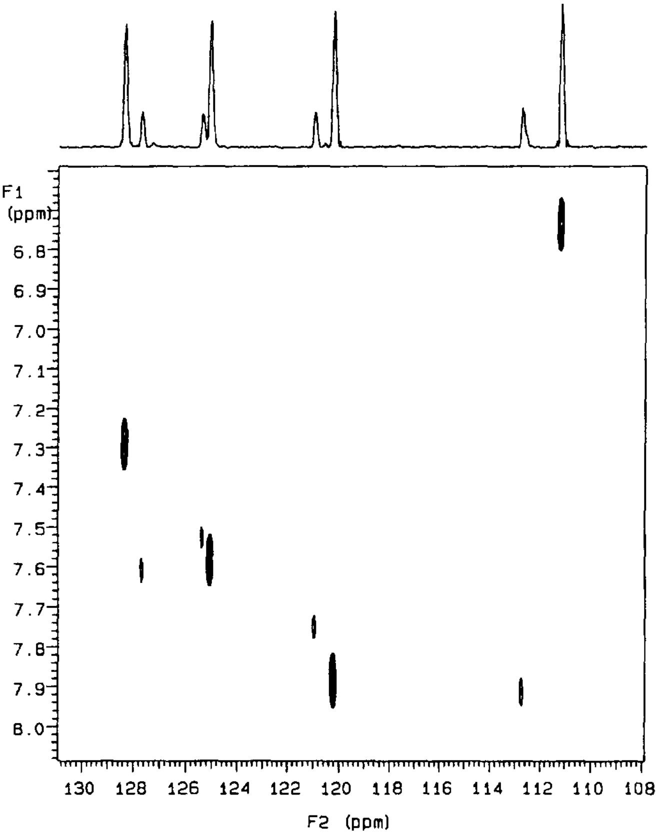

Figure 2. ^{13}C-^{1}H shift correlated 2D NMR spectrum of **3b**.

A possible explanation for this assumption might be the existence of a second conformer in which the benzene rings are more distant from each other. To investigate this possibility we performed high temperature molecular dynamics simulations of **3b**. The high temperature was chosen in order to pass high energy barriers between different conformations and hence to cover the whole conformational space. In fact, the visual inspection of the molecular dynamics run indicated interconversions between three different conformers. Two of them (a, c) are mirror images and correspond to the enantiomers found in the X-ray structure and the third (b) is the diastereomer. The latter is characterized by a syn-orientation of the disulfide linked benzohetaryl units, whereas the enantiomers have an anti-orientation of this structure element (Figure 3).

In the syn-conformer the H6 and H7 protons should not be influenced by the ring current of a neighbouring benzene ring which is in accord with our observations for the chemical shifts of the species **MI**. However, the high temperature, necessary to pass the energy barriers between the conformations, pointed to a rather improbable process (at lower MD temperatures no interconversions could be observed). This is underlined by the force field optimizations of the diastereoisomers yielding an energy difference of 12.4 kcal mol^{-1}. On the basis of this large energy difference, detection of the syn-conformer in the NMR experiment should be prevented, even if the calculations overestimate the energy gap.

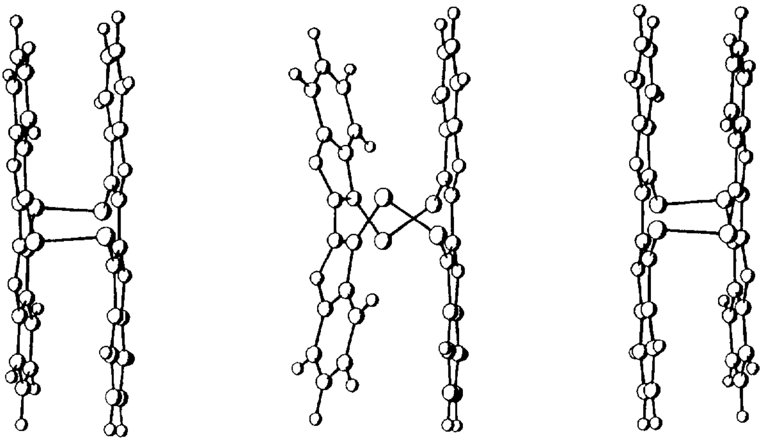

(a) (b) (c)

Figure 3. Plot drawing of the two enantiomers with *anti*-arrangement of the disulfide linkage (a, c) and the diastereomer (b) with the corresponding *syn*-orientation obtained from molecular mechanics calculations.

As already mentioned at the beginning, high temperature NMR measurements of **3b** indicated significant changes in the signal ratios of the species **MA** and **MI**. On gradual heating in a temperature range of 298 to 413 K the signal set of higher intensity (species **MA**) decreases and the signal set of lower intensity (species **MI**) increased (Figure 4). Upon cooling this process is reversible. However, no broadening of signals could be observed during the experiments. The lack of coalescence points to an equilibrium process between **MA** and **MI** which is relatively slow on the NMR timescale.[15]

Moreover, we could detect a concentration dependence of the signal ratios for the species **MA** and **MI**. We found signal ratios of 65:35, 74:26 and 78:22 for 1 mg, 2 mg and 3 mg solutions of **3b** in 1 ml HMPT-d_{18}. Since a conformational equilibrium, as depicted above, should not be affected by different concentrations an equilibrium between *chemically* different molecules must be responsible for this fact. Hence, an equilibrium between the 12-membered cyclic bis-disulfide **3b** and its monomer, the dithiine **2b**, seems to be the most probable explanation.[16]

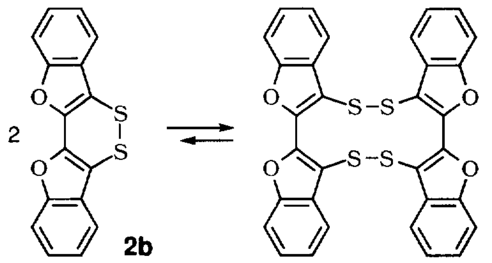

2b **3b**

This equilibrium also explains the chemical shift differences of the two species **MA** (dimer) and **MI** (monomer) observed in the ^{1}H NMR spectrum since the protons of the dithiine **3b** are not influenced by the ring current of a neighbouring benzene ring. The assumption of an equilibrium would be in agreement too with the absorption in the visible region (λ_{max} = 473 nm, lg ε = 3.26; $1.3 \cdot 10^{-4}$ molar, dichloromethane) which is characteristic of a 1,2-dithiine system.[17]

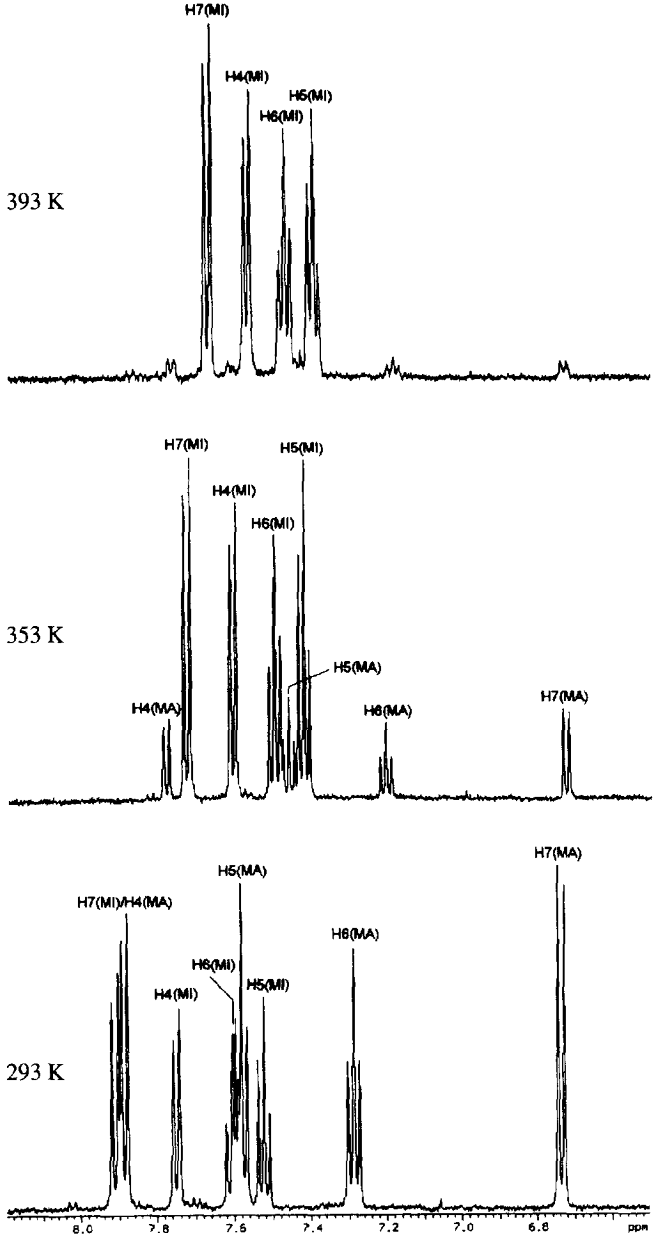

Figure 4. Variable temperature ^{1}H NMR measurements of **3b** in HMPT-d_{18}.

From the monomer-dimer ratios of the concentration dependence an equilibrium constant $K_c = 0.00035$ mol·l^{-1} can be calculated from equation (2)

$$K_c = \frac{c_{Mo}^2}{\left(c_0 - \frac{1}{2}c_{Mo}\right)} \qquad (2)$$

where c_0 and c_{Mo} are the initial molar concentration and the molar concentration of the monomer, respectively. The value of K_c shows that the equilibrium is shifted to the dimer at room temperature. From K_c a Gibbs free energy, ΔG°, of 4.7 kcal mol^{-1} was calculated.

The values of ΔG° together with that of ΔH° and ΔS° were determined by a linear regression analysis using the method of Booth[18] from the temperature dependent NMR spectra of **3b**. The monomer/dimer ratios were obtained by integration of the signals and subsequent conversion into the molar concentrations. The regression curve is shown in Figure 5 and an illustration of the corresponding concentrations of the monomer, and the dimer as a function of the temperature is given in Figure 6. From the regression analysis values of 10.7 kcal mol^{-1}, 20.6 cal mol^{-1} K^{-1} and 4.5 kcal mol^{-1} for ΔH°, ΔS° and ΔG°, respectively, were obtained. The ΔG° value, obtained in this way, is in good agreement with that gained from K_c. The positive sign of this ΔG° value indicates also a strong predominance of the dimer **3b** over the monomer **2b** in solution. The positive entropy term causes the Gibbs function changes to decrease appreciably with increasing temperature and hence the equilibrium is shifted to the monomeric dithiine **3b** (see Figure 6).

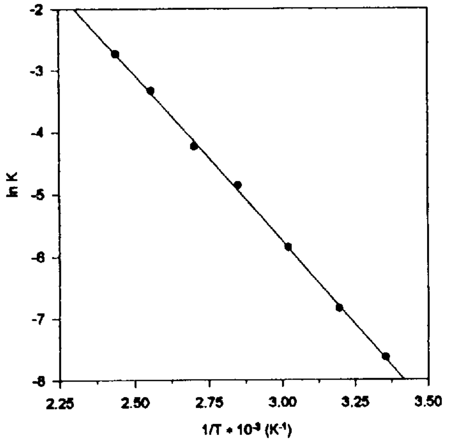

Figure 5. Temperature dependence of the equilibrium constant for **3b** $\rightleftharpoons$ 2 **2b**.

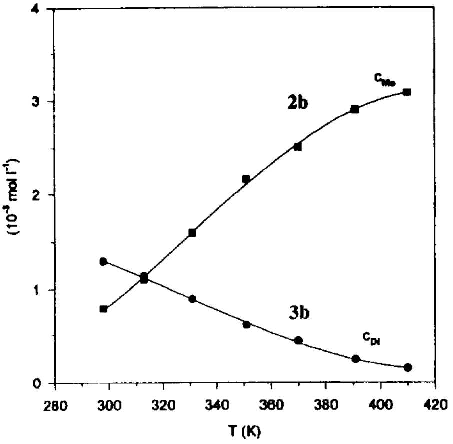

Figure 6. Monomer [c_{Mo} (**2b**)/dimer [c_{Di} (**3b**)] concentrations as a function of temperature.

These results are reinforced by the semiempirical calculations using the PM3 hamiltonian. From this differences in the heats of formation ($\Delta\Delta_B H$) of -0.8 kcal mol^{-1} and 8.9 kcal mol^{-1} were obtained for **3a**/2 **2a** and **3b**/2 **2b**, respectively. Since the entropy differences obtained from the PM3 calculations are very similar (ΔS = 41.61 cal mol^{-1} for **3a**/2 **2a** and 41.66 cal mol^{-1}) from the $\Delta\Delta_B H$ value of -0.8 kcal mol^{-1} and the experimentally obtained value ΔS° for **3a**/2 **2a** a ΔG° value of about -6.95 kcal mol^{-1} at 298 K can be extrapolated for the equilibrium of the benzo[b]thieno compounds **3a**/2 **2a**. This reflects the exclusive formation of the dithiine **2a** during the oxidation of **1a** and the lack of a second signal set in the room temperature NMR spectra. Even at extremely lower temperature there should be no significant dimer population. This is supported by NMR measurements of **3a** up to 183 K where no second set of signals was evident.

To determine the rates between the exchange of the aromatic proton signals of **3b** and **2b** we used ^{1}H two-dimensional NMR exchange spectroscopy (2D-EXSY) at a temperature of 303 K. Exchange cross peaks are clearly observed between the dimer and the monomer. The spectrum at 303 K is shown in Figure 7.

Analysis of the diagonal and cross-peak signal intensities were measured as volume integrals using the Varian standard software. The rate constant was calculated with equations (3) and (4) according to ref.[19],

$$k = \frac{1}{\tau_m}\ln\frac{r+1}{r-1} \qquad (3) \qquad\qquad r = \frac{4X_{Di}\cdot X_{Mo}\cdot\left(I_{AA}+I_{BB}\right)}{\left(I_{AB}+I_{BA}\right)-\left(X_{Di}-X_{Mo}\right)^2} \qquad (4)$$

where k is the exchange rate, τ_m corresponds to the mixing time, X_{Mo} and X_{Di} are the mole fractions and I_{AA}, I_{BB}, I_{AB}, I_{BA} are the intensities of the diagonal and cross peaks, respectively.

The value for this exchange is 0.33 s^{-1}; that is compatible with the fact that the monomer-dimer equilibrium does not proceed in the NMR timescale.

The mutual transformations between the monomeric and dimeric disulfides are not yet exactly understood. It is possible that a continuing energy costly torsion of the bis-disulfide **3b** until a minimal distance of

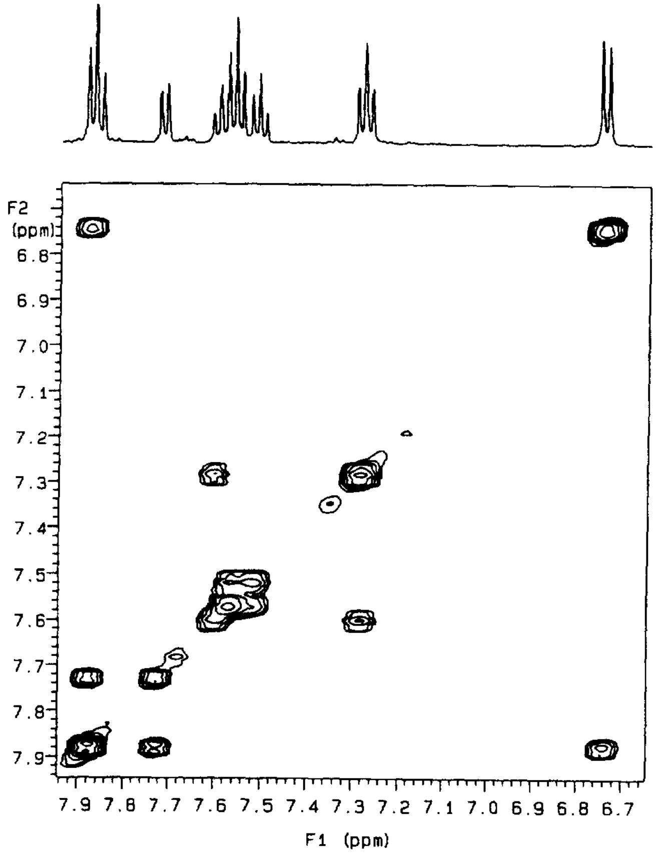

Figure 7. 2D-EXSY spectrum of **3b**/**2b** at 303 K.

the sulfur atoms S1 → S2a and S2 → S1a in Figure 1 is achieved may be a crucial requirement in the dissociation process. The difference in bond angles in the heterocyclic moiety resulting from the difference in heteroatom present in the anellated rings (**3a**/**2a** versus **3b**/**2b**) and steric factors are responsible for the position of equilibrium. Finally, the low solubility of the dimers **3** in all common solvents should be taken into account as the reason for the sole isolation of the compounds.

CONCLUSION

As previously stated, the oxidation of the "leuco" precursors affords either the 1,2-dithiines **2** (monomers) or the 12-membered cyclic bis-disulfides **3** (dimers) depending upon the nature of the anellated heterocyclic unit. Whilst the structure of **3** has been unequivocally established by X-ray crystallography, in solution NMR clearly indicates two sets of temperature dependent signals, which are not due to two different conformers. In the case of the benzo[b]furano anellated compound we conclude from NMR and molecular modelling studies that an equilibrium between **3b** and **2b** exists. However in the case of the benzo[b]thieno anellated compound only the 1,2-dithiine **2a** is present in solution and its dimer **3a** cannot be detected even at very low temperatures. The predominance of **3b** and **2a** is due to to enthalpy reasons. The monomer-dimer equilibrium has been characterized thermodynamically.

EXPERIMENTAL

Samples of **2a** and **3b** were prepared as described previously.[1a,3] The ^1H and ^{13}C NMR spectra were measured on a Varian Unity 500 spectrometer at frequencies of 499.84 MHz and 125.71 MHz, respectively, using 5 mm sample tubes. Compound **2a** was measured in $CDCl_3$ solution. Because of the extremely low solubility of **3b** in all common organic solvents, spectra for this compound were recorded in HMPT-d_{18}. However, the high melting point of this solvent precluded its use for low temperature measurements. Solutions for the measurements were prepared by dissolving 1-3 mg of **3b** in 1 ml HMPT-d_{18} (δ_H = 2.53 ppm, δ_C = 35.8 ppm). TMS was added for chemical shift reference. For the determination of the ^1H chemical shifts and H,H coupling constants the standard Varian NMR software including an iterative spin simulation program based on the LAOCOON program[20] was used.

Temperature control was achieved by using an Unity 500 temperature controller and calibrated by using the standard chemical shifts of glycol for high temperature and of methanol at low temperature, respectively. The spectra were measured in a temperature range of 183 to 303 K for **2a** and of 298 to 413 K for **3b**. The 2D NMR spectra were recorded using the standard Varian software. The 2D-EXSY data were collected in the phase sensitive mode (States-Haberkorn method)[21] using a 3s relaxation delay between repetition of the pulse sequence, an acquisition time of 0.225 s, a mixing time of 0.8 s, and a spectral width of 1100 Hz, an F_2 dimension of 2048 words and an F_1 dimension of 1024 words, zero filled to 2048 words, were used. The 2D spectra were processed using a shifted sinebell window function and left unsymmetrized.

The computational studies were carried out with the SYBYL 6.01 software[22] including the TRIPOS force field[23] running on a SGI Crimson Elan and an IBM RISC/6000 workstation. The force field optimization were performed using a distance-dependent dielectric with $\varepsilon = 1$ until the rms energy gradient was less than 0.001 kcal mol^{-1} $Å^{-1}$ using the Powell minimizer included in the SYBYL/MAXIMIN2 routine. The Gasteiger-Hückel method[24] was used for the calculation of the partial charge distribution of the molecules.

Molecular dynamics simulations were performed using the MD module of SYBYL. The system was equilibrated for 5 ps starting with random velocities. This was followed by 300 ps of MD at 2000 K with a time step of 1 fs and a data write frequency of 50 fs. The SHAKE procedure was applied to constrain all covalent bonds involving a hydrogen to their equilibrium length.

The semiempirical calculations were done using the PM3 method[25] included in MOPAC 6.0[26] and increased precision (keywords PRECISE, FORCE, THERMO(298) as well as ROT=2 for **3a,b** and ROT=4 for **2a,b**, respectively).

Acknowledgements: Financial support by the Fonds der Chemischen Industrie, Frankfurt/Main, and the Deutsche Forschungsgemeinschaft is acknowledged. We are indebted to Professors *S. Biali*, Jerusalem, *R. Radeglia*, Berlin, and *J. Sieler*, Leipzig, for helpful discussions. We are very grateful to Dr. A. Dunn, Frankfurt/Main, for editorial assistance.

REFERENCES AND NOTES

☆ Dedicated to Professor Richard R. Schmidt on the occasion of his 60th anniversary

1. cf.: a) Schroth, W.; Hintzsche, E.; Felicetti, M.; Spitzner, R.; Sieler, J.; Kempe, R. *Angew. Chem.* **1994**, *106*, 808-810; *Angew. Chem. Int. Ed. Engl.* **1994**, *33*, 739-741 and literature cited therein. – b) Schroth, W.; Felicetti; M.; Hintzsche, E.; Spitzner, R; Pink, M. *Tetrahedron Lett.* **1994**, *35*, 1977-1980.
2. a) Gompper, R.; Hartmann, K.; Polborn, K. *Tetrahedron Lett.* **1994**, *35*, 1994, 9195-9196. – b) cf. also: Glas, G.; Gompper, R.; Junius, M.; Mertz, R.; Wagner, H.-U.; Nöth, H.; Staudigl, R. *J. Prakt. Chem.* **1990**, *332*, 949-967.
3. a) Schroth, W.; Hintzsche, E.; Viola, H.; Winkler, R.; Klose, H.; Boese, R.; Kempe, R.; Sieler, J. *Chem. Ber.* **1994**, *127*, 401-408. – b) cf. also: Hartmann, H.; Scheithauer, S. *J. Prakt. Chem.* **1969**, *311*, 827-843.
4. Tables of the atomic coordinates, thermal parameters, bond lengths, and angles have been deposited at the Cambridge Data Centre, University Chemical Laboratory, Lensfield Road, Cambridge CB2 1EW. The X-ray data are available on request from the Director of the CCDC by quoting the full literature citation of this paper.

5. Crystal data: $C_{32}H_{16}O_4S_4$ (592.69); orthorhombic; space group Fdd2; a = 13.410(2), b = 34.062(4), c = 23.504(2) Å, $\alpha = \beta = \gamma = 90°$; V = 10736(2) $Å^3$; 16 molecules per unit cell; 3760 unique reflections were measured (diffractometer STADI4 [Stoe], MoK_α radiation, $3 < 2\Theta < 54°$). The structure was refined by a full-matrix least squares method (SHELXL 93). R-values: $R_1 = 0.0355$, $R_2 = 0.0657$ for reflections with $[I > 2\ \sigma(I)]$ and $R_1 = 0.1857$ and $wR_2 = 0.0802$ for all data.
6. For the X-ray analysis of **2a** see ref.[3a].
7. cf.: a) Chen, C. W.; Whitlock Jr., H. W. *J. Am. Chem. Soc.* **1978**, *100*, 4921-4922. – b) Weber, E.; Vögtle, F. *Chem. Unserer Zeit* **1989**, *23*, 210-211; and literature cited therein.
8. cf.: Sijbesma, R. P.; Kentgens, A. p. M.; Lutz, E. T. G.; van der Maas, J. H.; Nolte, R. J. M. *J. Am. Chem. Soc.* **1993**, *115*, 8999-9005.
9. For a review on the stereochemistry of disulfides see: Rahman, R.; Safe, S.; Taylor, A. *Q. Rev., Chem. Soc.* **1970**, *24*, 208-237.
10. a) Lüttringhaus, A.; Hess, D.; Rosenbaum, H. J. *Z. Naturf., Teil B*, **1967**, *22*, 1296-1300. – b) Lüttringhaus, A.; Rosenbaum, H. J. *Monatsh. Chem.* **1967**, *98*, 1323-1331.
11. Guttenberger, H. G.; Bestmann, H. J.; Dickert, F. L.; Jørgensen, F. S.; Snyder, J. P. *J. Am. Chem. Soc.* **1981**, *103*, 159-168.
12. Geneste, P.; Olivé, J.-L.; Ung, S. N.; El Faghi, M. E. A.; Easton, J. W.; Beierbeck, H.; Saunders, J. K. *J. Org. Chem.* **1979**, *44*, 2887-2892.
13. Elgamal, M. H. A.; Elewa, N. H.; Elkhrisy, E. A. M.; Duddek, H. *Phytochem.* **1979**, *18*, 139-143.
14. Günther, H.; NMR-Spektroskopie, 3rd edition, Georg Thieme Verlag, Stuttgart, New York, **1992**; p.84.
15. For a further example of the lack of coalescence in variable temperature NMR measurements see: Jancke, H.; Radeglia, R.; Tresselt, D.; Berg, H. *Z. Chem.* **1977**, *17*, 105-106.
16. In the case of the less soluble **3**, X = N-Me, *three* sets of signals occur in a more complicated arrangement with reversible temperature dependence of the intensities (^1H and ^{13}C NMR [HMPT-d_{18}]; cf. ref.[1a], there table 1). Between two (overlapped) sets coalescence is indeed evident on increasing temperature, possibly due to steric reasons from the Me groups (existence of different conformers within the NMR timescale).
17. a) It should be emphasized, however, that **3b** forms also red crystals; for specifications see ref.[1a]. – b) Concerning the absorption of 1,2-dithiines in the visible region cf.: Schroth, W.; Billig, F.; Langguth, H. *Z. Chem.* **1965**, *5*, 353-354. – Schroth, W.; Billig, F.; Reinhold, G. *Angew. Chem.* **1967**, *79*, 685-686; *Angew. Chem. Int. Ed. Engl.* **1967**, *6*, 698-699. – Borsdorf, R.; Hofmann, H.-J.; Scholz, M.; Fabian, J. *Tetrahedron* **1970**, *26*, 3227-3231. – Fabian, J.; Birner, P. *Coll. Czech. Chem. Commun.* **1988**, *53*, 2096-2115. – Cimiraglia, R.; Fabian, J.; Hess Jr., B. A. *J. Mol. Struct.*, **1991**, *230*, 287-293.
18. Booth, H. *Kem.-Kemi* **1980**, *7*, 5-10.
19. Perrin, C. L.; Dwyer, T. J. *Chem. Rev.* **1990**, *90*, 935-967.
20. Castellano, S.; Bothner-By, A. A. *J. Chem. Phys.* **1964**, *41*, 3863-3869.
21. States, D. J.; Haberkorn, R. A.; Ruben, D. J. *J. Magn. Reson.* **1982**, *48*, 286-292.
22. SYBYL version 6.01, Tripos Associates, Inc.,St. Louis, MO 63144.
23. Clark, M.; Cramer, R. D.; van Opdenbosch, N. *J. Comput. Chem.* **1989**, *10*, 982-1012.
24. Gasteiger, J.; Marsili, M. *Tetrahedron* **1980**, *36*, 3219-3226. – M. Marsili, Gasteiger, *J. Croat. Chem. Acta* **1980**, *53*, 601-614.
25. Stewart, J. J. P.; *J. Comput. Chem.* **1989**, *10*, 209-220, 221-264.
26. MOPAC, program number 455, available from the Quantum Chemistry Program Exchange at Indiana University.

(*Received in Germany* 2 *May* 1995; *accepted* 16 *June* 1995)